Geometrical Frustration in Amorphous and Partially Crystallized Packings of Spheres

N. Francois,* M. Saadatfar,† R. Cruikshank, and A. Sheppard

Department of Applied Mathematics, Research School of Physics and Engineering, The Australian National University, Canberra, Australian Capital Territory 0200, Australia

(Received 16 March 2013; revised manuscript received 28 July 2013; published 2 October 2013)

We study the persistence of a geometrically frustrated local order inside partially crystallized packings of equal-sized spheres. Measurements by x-ray tomography reveal previously unseen grain scale rearrangements occurring inside large three-dimensional packings as they crystallize. Three successive structural transitions are detected by a statistical description of the local volume fluctuations. These compaction regimes are related to the disappearance of densely packed tetrahedral patterns of beads. Amorphous packings of monodisperse spheres are saturated with these tetrahedral clusters at Bernal's limiting density ($\phi \approx 64\%$). But, no periodic lattice can be built upon these patterns; they are geometrically frustrated and are thus condemned to vanish while the crystallization occurs. Remarkably, crystallization-induced grain rearrangements can be interpreted in terms of the evolution of key topological features of these aggregates.

DOI: 10.1103/PhysRevLett.111.148001 PACS numbers: 61.43.−j, 05.65.+b, 45.70.−n, 81.10.Aj

The structural organization of dense materials such as granular matter, glass, colloids, and some metals is naturally built upon local patterns that cannot tile the space, a phenomenon known as *geometrical frustration* [1–3]. Applying external forces can cause these complex structures to rearrange into periodic crystals, leading to dramatic alterations of their physical properties [4]. How these substantial morphological changes occur during crystallization is often difficult to describe [5]. Dense packings of identical spheres are commonly used to model complex frustrated structures as well as global ordering transitions [6]. However, our understanding of the crystallization of densely packed athermal spheres remains largely incomplete. The nature of the structural inhibition which prevents disordered packings of equal-sized spheres from being denser than 64%, the random close packing (rcp) limit, is highly debated [7–12]. Moreover, frictional packings need to be strongly vibrated or sheared to pass the density of 64%, and crystalline clusters inevitably appear [13–15]. An entropic mechanism driving this ordering despite the highly dissipative context has yet to be found [16–18].

As a packing crystallizes, it undergoes major grain-scale rearrangements. A clear geometrical description of these rearrangements could represent a first step towards the elaboration of a statistical framework for granular crystallization [13,19]. This challenging approach relies on finding key patterns characterizing amorphous states and on describing their evolution while the packing crystallizes.

In the 1960s, J. D. Bernal's pioneering effort to model the structure of simple liquids as "heaps of spheres" led him to two breakthroughs. He first noticed the predominance of local tetrahedral configurations in disordered sphere packings. Then, he described the propensity of these tetrahedra to pack via their faces to form dense *polytetrahedral* aggregates [6]. Such polytetrahedral arrangements can produce a rich range of motifs [20], but none can periodically tile the space; i.e., they are geometrically frustrated patterns [6,21]. The densest local arrangement, the icosahedron, is often used to explain the existence of disordered structures [1]. Yet, recent computer models on frictionless packings [13] emphasize that polytetrahedral aggregates are naturally composed of linear branches connecting ring structures which contain five tetrahedra (five-rings). Moreover, it has been suggested that the rcp state is saturated with dense polytetrahedral clusters, such that any further densification involves the presence of crystalline configurations. This tantalizing proposition gives a clear geometrical principle on which both the rcp limit and the crystallization could eventually be statistically understood for monodisperse sphere packings [13]. There is as yet no experimental study giving a quantitative picture of the topology of the polytetrahedral structures or describing the fate of these aggregates beyond the rcp bound.

Here, we use a combination of novel experiments, x-ray computed tomography, and statistical and topological analysis to investigate the structure of frictional packings before the rcp limit and far beyond in the crystalline region. At $\phi \approx 64\%$, crystalline clusters inevitably appear in these highly monodisperse packings, and this emerging order enforces a sharp transition in the packing polytetrahedral structure. Our analysis of the polytetrahedral clusters shows that branches of tetrahedra and five-ring structures are key topological features whose evolution is directly related to successive crystallization regimes revealed by the local volume fluctuations.

Our experimental setup extends vibrating techniques used to study the compaction of amorphous packings [14,22]. To observe a massive crystallization under vibrations, the experiments are performed with monosized acrylic beads (diameter = 1 mm, polydispersity = 2.5%)

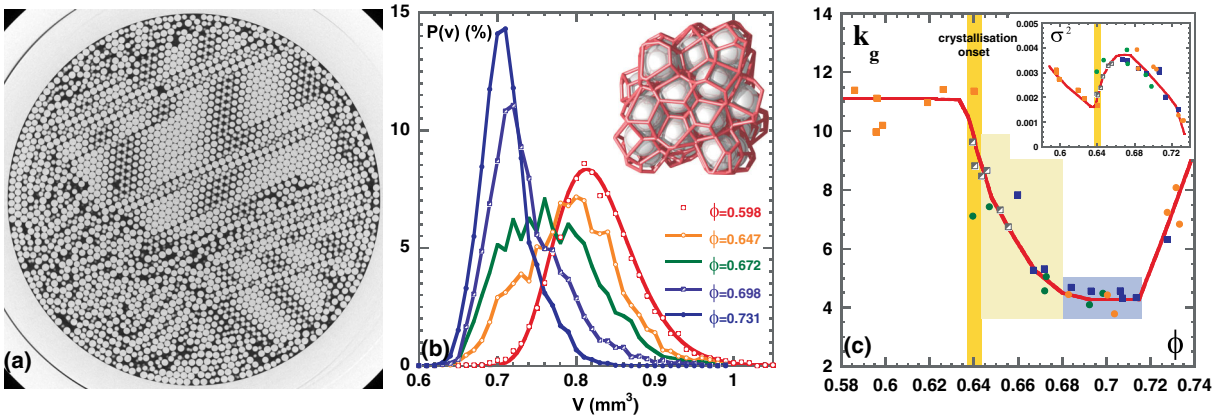

FIG. 1 (color online). (a) Tomographic slice of a partially crystallized packing ($\phi \approx 70.5\%$) in a spherical container. (b) PDF of the local volume fluctuations for increasing global volume fraction ϕ. The PDF for $\phi = 0.598$ is fitted by a gamma distribution (red line). Inset: The Voronoi partition of a local configuration of beads. The bead and the surrounding space closest to its center define the Voronoi elementary brick. (c) The granular "specific heat" $k_g = (\bar{V} - V_{\min})^2/\sigma^2$ versus ϕ. Three successive transitions are highlighted at $\Phi = 0.64$, 0.68, 0.72. 34 subsets [26] of roughly 4000 beads extracted from six different packings (indicated by different markers) have been analyzed: two initial jammed packings obtained by pouring + four partially crystallized packings. Inset: Variance σ^2 of the Voronoi volume versus ϕ.

which are packed into large cylindrical or spherical containers (inner diameter = 66 mm). A batch of approximately 200 000 beads is poured into the container forming an initial packing in a random configuration with a volume fraction ϕ ranging from 57% to 63%. The packings are then shaken intensely for few seconds, to the point of fluidization [14], where a fast compaction is observed. The resulting global packing density ranges from 68.5% up to 71.5%. The internal structure of these packings is imaged by means of x-ray computed tomography (see Refs. [23,24] and the Supplemental Material [25]). Figure 1(a) shows a tomographic slice of a dense packing obtained in a spherical geometry. The heterogeneous structure of the packing is evident with disordered domains ($\phi \approx 0.65$) coexisting with large and almost perfectly crystalline clusters ($\phi \approx 0.732$). We have consistently obtained such partially crystallized packings, whose statistical and topological features primarily depend on ϕ regardless of the initial jammed configuration or the container geometry. Our analyses have been carried out on global packings as well as subsets containing 4000 spheres [26].

To explore how local configurations become denser during the crystallization, we divide the packing according to the Voronoi tessellation [inset of Fig. 1(b)]. This grain-centered partitioning allows us to estimate the probability distribution function (PDF) of the local volume fluctuations and their statistics: i.e., its variance σ^2, mean value $\bar{V}$, and minimal bound $V_{\min}$.

Figure 1(b) shows such a PDF for decreasing global volume fraction. The PDF for disordered packings ($\phi < 0.64$) is asymmetric and corresponds to a gamma law whose variance decreases with compaction [inset of Fig. 1(c) and Ref. [27]]. In the density range $\phi \in [0.64, 0.68]$, although the global volume fraction decreases ($\bar{V}$ decreases), the PDF flattens and its variance increases. Beyond $\phi \approx 0.68$, it gets narrower and peaks around $V = 0$, 71 mm^3, which corresponds to cubo-octahedral crystalline configurations.

An intensive granular variable $kg = (\bar{V} - V_{\min})^2/\sigma^2$ has recently been suggested as granular material's equivalent of "specific heat" [27]. kg should therefore be a measure of structural rearrangements probed over the local volume fluctuations. This parameter reveals three successive transitions occurring in our packings at $\Phi \approx 0.64$, 0.68, and 0.72, as shown in Fig. 1(c). The sharp drop observed at $\Phi \approx 0.64$ is related to the onset of crystallization, which was detected by a bond order parameter method (see Ref. [28] and the Supplemental Material [25]). The two subsequent regimes of compaction at higher densities ($\phi > 0.68$) are in contrast with the monotonic drop of kg reported in numerical simulations [27]. These transitions might be connected to global transformations of the growing crystalline clusters [28,29].

To reveal grain rearrangements associated with these structural transitions, we now describe packings in terms of the simplices (generalized tetrahedra) of the Delaunay partition [inset of Fig. 2(a)] [30]. Since Bernal's work, it is known that clusters made of quasiregular tetrahedra play a major role in the structure and compaction of disordered packings [6,13,19].

These tetrahedral patterns are revealed within the Delaunay partition through two working hypotheses. (i) A simplex is considered dense (or quasiregular) if its longest edge l is smaller than 5/4 of the diameter d of the beads that compose the simplex. Dense simplices for which ($\delta = l - d \leq 0.25 \times d$) will be called tetrahedra [6,13]. (ii) In an assembly of tetrahedra, those who share a face show a greater mechanical stability than tetrahedra

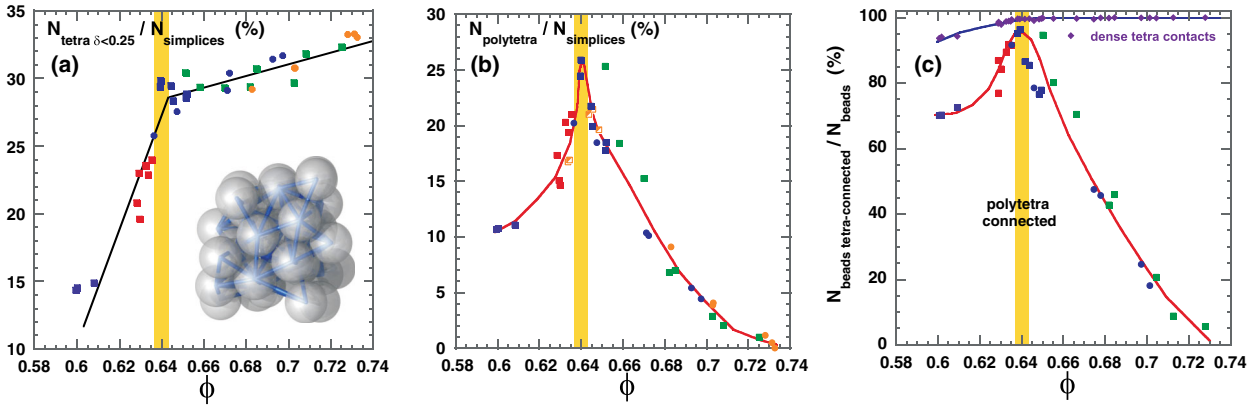

FIG. 2 (color online). Evolution of the densest simplices (quasiregular tetrahedra) of the Delaunay tessellation versus the volume fraction. (a) Fraction of tetrahedra ($\delta < 0.25 \times d$) versus ϕ. Inset: The Delaunay representation of a local configuration of beads. It is based on local simplices (generalized tetrahedra) built on the centers of the locally four closest beads. (b) Fraction of tetrahedra that are face adjacent and are involved in aggregates (polytetrahedral clusters) containing more than 3 components. (c) Fraction of beads which are part of at least one dense tetrahedron (blue line) or that are part of a polytetrahedral cluster (red line).

connected by an edge or a vertex. Stable *polytetrahedral* aggregates are defined as clusters made of three or more face-adjacent tetrahedra. These clusters are frustrated structures which cannot be part of any periodic crystalline lattice [1,19]. Conversely, isolated pairs of face-adjacent tetrahedra are found in the hcp crystal.

Figure 2 shows some characteristics of polytetrahedral clusters for $\phi \approx 0.59$ up to $\phi \approx 0.73$. The number of tetrahedra [Fig. 2(a)] and polytetrahedral clusters [Fig. 2(b)] increases sharply as random packings get denser. The fraction of polytetrahedral clusters has a pronounced maximum around $\phi \approx 0.64$ [Fig. 2(b)]. At this peak, almost all the tetrahedra are involved in a frustrated cluster. Beyond $\phi \approx 0.64$, polytetrahedral clusters fade away progressively. At $\phi \approx 0.64$, all the beads are involved in a dense tetrahedron and are thus in ''contact'' with a polytetrahedral structure [Fig. 2(c)]. These polytetrahedral contacts are gradually replaced by crystalline contacts beyond the rcp limit. However, the Delaunay mapping associates many tetrahedra to each bead; thus, even at $\phi \approx 0.68$, a small fraction of polytetrahedral aggregates (7%) still involves a large number of beads (40%). Moderate modifications of the condition ($\delta < 0.25 \times d$) leave the global picture qualitatively unchanged [19].

Our experiments confirm two features observed in numerical modeling of frictionless packings [13]: an increasing fraction of polytetrahedral clusters provides a densification mechanism for disordered packings, and this densification process is limited by the rcp density where the fraction of beads free to be part of a cluster is exhausted. Remarkably, this scenario, based on pure geometrical features, seems to be common to both frictionless and dissipative structures. Beyond Bernal's limit ($\phi \approx 0.64$), monodisperse sphere packings inevitably start crystallizing. The existence of a sharp maximum in Fig. 2(b) is a signature of this abrupt crystallization onset which insures the uniqueness of the rcp limit (as opposed to a J line [9,12]). However, a significant number of polytetrahedral clusters survives beyond $\phi \approx 0.64$ [Figs. 2(b) and 2(c)].

A polytetrahedral cluster can be viewed as a network in which each vertex is a dense tetrahedron and each bond is made by two tetrahedra sharing a face. Figure 3 shows some features of this network for $\phi \approx 0.64$. Bonds are formed in a complex manner that sometimes creates closed loops. These loops are named rings; many rings consist of five tetrahedra (named five-rings) [Figs. 3(a)–3(c)]. We use a network analyzer to describe the topology of these structures (see the Supplemental Material [25]).

The population of face-adjacent tetrahedra is sorted according to three key topological features: tetrahedra forming a ring structure, tetrahedra from polytetrahedral clusters that are not involved in a ring and are called branched tetrahedra, and pairs of tetrahedra (bipyramids). Rings and branched tetrahedra compose the frustrated polytetrahedral family which is condemned to disappear during crystallization [1]. Figure 4(a) shows the evolution versus ϕ of these topological descriptors.

Beyond $\phi \approx 64\%$, the increasing fraction of bipyramids discloses the growth of hcp crystalline structures. The presence of bipyramids below the rcp density may play a role in the slow compaction dynamics of amorphous packings, as reported for colloidal glass [31].

Below the rcp limit, $\approx 2/3$ of the polytetrahedral clusters are made of branched tetrahedra. This fraction decreases continuously with density increase. However, these motifs are resilient features which survive for $\phi \geq 68\%$ when rings have almost disappeared. In this regime, a large amount of beads ($\approx 40\%$) is still connected via these linear patterns [Fig. 2(c)]. These branched tetrahedra eventually vanish for $\phi \geq 72\%$–73% [Figs. 2(b) and 4(a)].

Conversely, the evolution of the ring fraction is not monotonic but peaks around the rcp density. Below

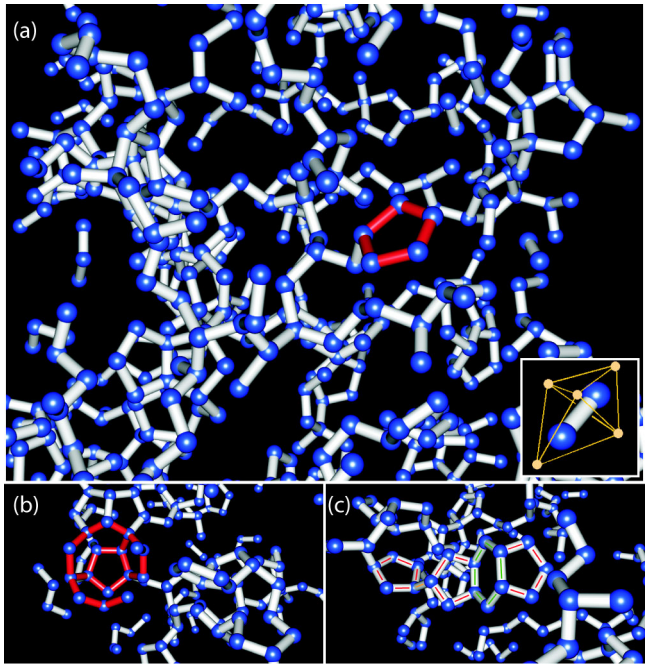

FIG. 3 (color online). Visualizations of the topology of polytetrahedral aggregates. Polytetrahedral clusters are represented as networks in which each vertex (blue sphere) is a dense tetrahedron and each bond (white tube) represents two tetrahedra sharing a face. The inset of (a) shows the centers of beads forming a pair of face-adjacent dense tetrahedra and their topological representation. (a) Polytetrahedral clusters in a packing at $\phi \approx 0.64$. A loop composed of five face-adjacent tetrahedra (five-ring) is highlighted in red. (b) Close-up on an "incomplete" icosahedral configuration. A cluster of 12 five-rings would form an icosahedron; here, this structure contains two five-rings adjacent to an eight-ring. (c) Close-up on a "chain" of rings composed of five-rings (red lines) and a six-ring (green lines).

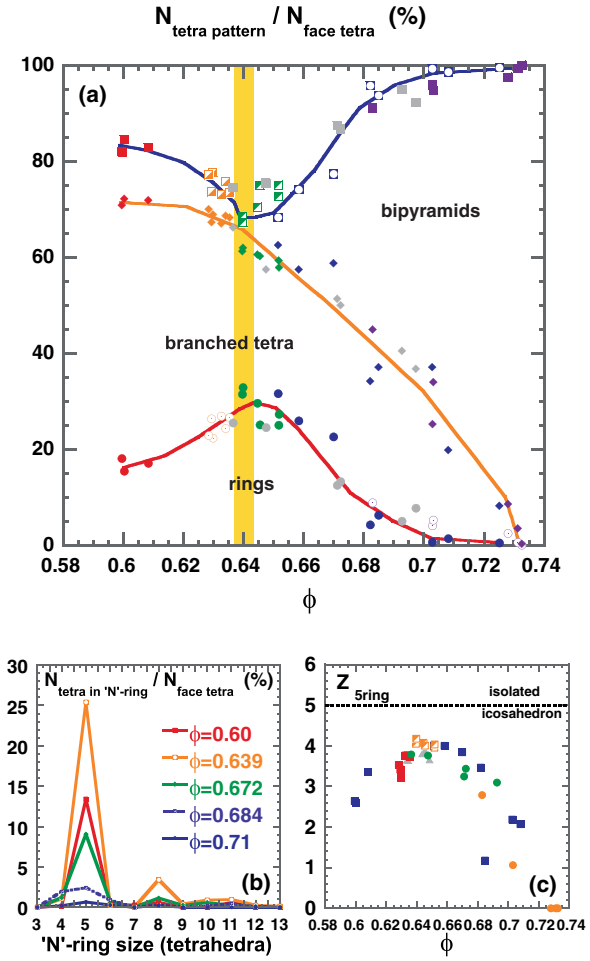

FIG. 4 (color online). (a) Evolution of the polytetrahedral topological classes versus the volume fraction. Tetrahedra involved in rings (red line, N_{rings}) and branched tetrahedra (orange line, N_{branched}) form the polytetrahedral family $N_{\text{polytetra}} = N_{\text{rings}} + N_{\text{branched}}$; the fraction of tetrahedra in bipyramids (N_{bipyr}) is the difference between the orange and the blue lines. The fractions are normalized by the number of face-adjacent tetrahedra $N_{\text{facetetra}} = N_{\text{polytetra}} + N_{\text{bipyr}}$. (b) Size distribution (in tetrahedra) of the ring patterns normalized by $N_{\text{facetetra}}$. (c) Outgoing average connectivity of the five-rings (see the Supplemental Material [25]); this connectivity is five for a five-ring part of an isolated icosahedron.

$\phi \approx 64\%$, a disordered packing becomes denser by forming an increasing fraction of rings which are mainly five-rings [Figs. 4(a) and 4(b)]. While this compaction mechanism peaks around $\phi \approx 64\%$, five-ring patterns still account for almost 80% of the tetrahedra involved in a ring structure up to $\phi \approx 68\%$ [Fig. 4(b)]. Although a persistent fivefold local symmetry is often reported to coexist with crystalline clusters, its role in crystal growth and morphology remains debated [29,32–34].

Beyond $\phi \approx 64\%$, five-rings disappear at 7 times the rate of branched tetrahedra. Their fraction falls below 2% at $\phi \approx 0.68$ [Fig. 4(b)] while branched tetrahedra still represent approximately half of the face-adjacent tetrahedra [Fig. 4(a)]. This salient decrease coincides with an increase in the local volume fluctuations [inset of Fig. 1(c)], a remarkable fact since the global volume fraction decreases. It signals that substantial grain rearrangements occur until five-rings almost vanished for $\phi \geq 68\%$ [Fig. 4(b)]. Five-rings are thus prime patterns to describe some crystallization rearrangements. Here, we show that (i) the rcp density is a fully frustrated limit showing a maximum of dense five-ring configurations, and (ii) the transition observed at $\phi \approx 68\%$ [Fig. 1(c)] corresponds to five-ring disappearance.

Beyond $\phi \approx 0.68$, the vanishing of branched patterns seems to induce fewer grain disturbances, since local volume fluctuations decrease again [inset of Fig. 1(c)]. In the range $\phi \in [0.68, 0.72]$, the decreasing variance of these fluctuations follows $\sigma^2 \approx (\bar{V} - V_{\text{min}})^2$, resulting in a plateau behavior for kg [Fig. 1(c)].

A polygonal cluster made of 12 five-rings forms an icosahedral configuration. The presence of a local icosahedral order is often invoked to explain the existence of disordered packings [1]. Figure 4(c) shows that five-ring

averaged outgoing connectivity $Z_{\text{five-rings}}$ is always smaller than 5 for any volume fractions, but $Z_{\text{five-rings}}$ is five for an isolated icosahedron. Besides, five-rings rarely aggregate into dense clusters. The densest configurations are related to a small fraction of eight-rings observed at $\phi \approx 64\%$ [Fig. 4(b)]. Those eight-rings are parts of incomplete icosahedral configuration [Fig. 3(b)]. Thus, five-rings do not aggregate to form icosahedral clusters. They are most likely connected to each other via branches of tetrahedra [Fig. 3(a)]. Despite the significant amount of distortion allowed ($\delta \leq 0.25 \times d$), the absence of icosahedral arrangements suggests that not all polytetrahedral structures are equally frustrated [21].

Since our packings are shaped by a strong fluidization process, these findings might be relevant for complex granular or suspension rheology issues [35,36]. Recent advances point out the importance of the network of enduring contacts for determining nonlocal constitutive laws of dense granular flows [36]. In monodisperse granular materials, polytetrahedral clusters might partially map onto this contact network and could enlighten the spatial organization of the mechanical backbone [37]. Interestingly, a transition in the mechanical coordination number of packings has recently been reported to occur for $\phi \in [0.64, 0.68]$ [12].

In conclusion, the disappearance of polytetrahedral clusters is an intrinsic geometrical feature of the crystallization of monodisperse frictional sphere packings. The evolution of key polytetrahedral patterns during the crystallization improves our understanding of the different structural transitions observed in the local volume fluctuations. The propensity of tetrahedra to coalesce via their faces might be interpreted as the existence of a directional entropic force [5]. It gives hope for the elaboration of a statistical framework for granular crystallization and related transitions observed in complex materials.

We thank S. Ramsden for the networks visualizations and M. Driol, E. Franklin, T. Aste, and T. Senden for their support.

*nicolas.francois@anu.edu.au
†mos110@physics.anu.edu.au

[1] J.-F. Sadoc and R. Mosseri, *Geometrical Frustration* (Cambridge University Press, Cambridge, England, 1999).
[2] L. Berthier and G. Biroli, Rev. Mod. Phys. **83**, 587 (2011).
[3] S. Fischer, A. Exner, K. Zielske, J. Perlich, S. Deloudi, W. Steurer, P. Lindner, and S. Frster, Proc. Natl. Acad. Sci. U.S.A. **108**, 1810 (2011).
[4] R. G. Larson, *The Structure and Rheology of Complex Fluids* (Oxford University, New York, 1998).
[5] P. F. Damasceno, M. Engel, and S. C. Glotzer, Science **337**, 453 (2012).
[6] J. D. Bernal, Proc. R. Soc. A **280**, 299 (1964).
[7] S. Torquato, T. M. Truskett, and P. G. Debenedetti, Phys. Rev. Lett. **84**, 2064 (2000).
[8] G. Parisi and F. Zamponi, Rev. Mod. Phys. **82**, 789 (2010).
[9] P. Chaudhuri, L. Berthier, and S. Sastry, Phys. Rev. Lett. **104**, 165701 (2010).
[10] S. C. Kapfer, W. Mickel, K. Mecke, and G. E. Schröder-Turk, Phys. Rev. E **85**, 030301 (2012).
[11] C. Song, P. Wang, and H. A. Makse, Nature (London) **453**, 629 (2008).
[12] Y. Jin and H. A. Makse, Physica (Amsterdam) **389A**, 5362 (2010).
[13] A. V. Anikeenko and N. N. Medvedev, Phys. Rev. Lett. **98**, 235504 (2007).
[14] P. Philippe and D. Bideau, Phys. Rev. Lett. **91**, 104302 (2003).
[15] K. E. Daniels and R. P. Behringer, Phys. Rev. Lett. **94**, 168001 (2005).
[16] J. S. Olafsen and J. S. Urbach, Phys. Rev. Lett. **95**, 098002 (2005).
[17] F. Pacheco-Vázquez, G. A. Caballero-Robledo, and J. C. Ruiz-Suárez, Phys. Rev. Lett. **102**, 170601 (2009).
[18] P. M. Reis, R. A. Ingale, and M. D. Shattuck, Phys. Rev. Lett. **96**, 258001 (2006).
[19] A. V. Anikeenko, N. N. Medvedev, and T. Aste, Phys. Rev. E **77**, 031101 (2008).
[20] A. Haji-Akbari, M. Engel, A. S. Keys, X. Zheng, R. G. Petschek, P. Palffy-Muhoray, and S. C. Glotzer, Nature (London) **462**, 773 (2009).
[21] J. A. van Meel, D. Frenkel, and P. Charbonneau, Phys. Rev. E **79**, 030201 (2009).
[22] P. Richard, M. Nicodemi, R. Delannay, P. Ribiere, and D. Bideau, Nat. Mater. **4**, 121 (2005).
[23] T. Aste, M. Saadatfar, and T. J. Senden, Phys. Rev. E **71**, 061302 (2005).
[24] T. Varslot, A. Kingston, G. Myers, and A. Sheppard, Med. Phys. **38**, 5459 (2011).
[25] See Supplemental material at http://link.aps.org/supplemental/10.1103/PhysRevLett.111.148001 for details regarding the experimental setup, the image analysis, the bond order parameter method, and the topological analysis of the polytetrahedral clusters.
[26] To reduce boundary effects, the analysis was performed over an inner region four sphere diameters away from the container boundary [23]. The subsets are nonoverlapping and were picked randomly in this inner region.
[27] T. Aste and T. Di Matteo, Phys. Rev. E **77**, 021309 (2008).
[28] B. A. Klumov, S. A. Khrapak, and G. E. Morfill, Phys. Rev. B **83**, 184105 (2011).
[29] A. V. Anikeenko, N. N. Medvedev, A. Bezrukov, and D. Stoyan, J. Non-Cryst. Solids **353**, 3545 (2007).
[30] T. Aste, Phys. Rev. Lett. **96**, 018002 (2006).
[31] M. Leocmach and H. Tanaka, Nat. Commun. **3**, 974 (2012).
[32] N. Ch. Karayiannis, R. Malshe, J. J. de Pablo, and M. Laso, Phys. Rev. E **83**, 061505 (2011).
[33] B. O'Malley and I. Snook, Phys. Rev. Lett. **90**, 085702 (2003).
[34] H. Shintani and H. Tanaka, Nat. Phys. **2**, 200 (2006).
[35] F. Boyer, E. Guazzelli, and O. Pouliquen, Phys. Rev. Lett. **107**, 188301 (2011).
[36] Y. Forterre and O. Pouliquen, Annu. Rev. Fluid Mech. **40**, 1 (2008).
[37] M. Saadatfar, N. Francois, A. Arad *et al.*, SEG Tech. Prog. Expan. Abst. **2012**, 1 (2012).